Supplementary Materials for “An Echelon-based Single Shot Optical and Terahertz Kerr Effect Spectrometer"

Authors: Griffin Mead, Ikufumi Katayama, Jun Takeda, Geoffrey A. Blake*

*Corresponding author: gab@gps.caltech.edu

Contents of Supplementary Materials:

A. Echelon Imaging

Properly imaging the echelon surface onto the camera array is critical for accurate measurements. The following example demonstrates how the echelon image is propagated along the optical path, and extensively uses the imaging equation

$$\frac{1}{fx} = \frac{1}{Ox} + \frac{1}{Ix} \tag{1}$$

The echelon surface plane is the first object O1 in the imaging pathway (Fig. 1 (a)). Light passing through the first lens L1 (focal length f1 = 200 mm) produces the first image I1 at a distance provided by the imaging equation. This image acts as the second object O2 for the second lens L2. The O2 distance from L2 must account for the 140 mm separation between L1 and L2. The remainder of the imaging pathway follows from this same procedure of propagating images along the optical path.

As the light passes through each lens, the images formed will change size. While the spherical lenses L1 and L2 uniformly change the horizontal and vertical dimensions of the image, the cylindrical lenses L3 and L4 are used to adjust the image magnification along a single axis. The L3 cylindrical lens forms image I3, and de-magnifies the horizontal axis of the echelon image. Similarly, the L4 cylindrical lens de-magnifies the vertical axis. The initial and final dimensions of the echelon object and images are shown in Fig 1 (b). Only a central slice of the final image is acquired by the active sub-array on the camera, as shown (c).

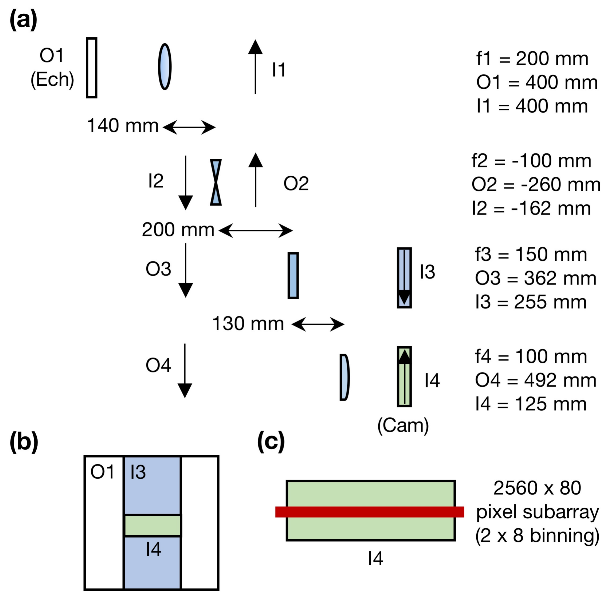

FIG. 1. (a) The location of the echelon image is followed through the optical path between the echelon surface and the camera array. (b) The relative size of the original echelon object (O1) and the images formed after the two cylindrical lenses L3 and L4 (I3 and I4 respectively). (c) A schematic comparison of the size of final image I4 and the active sub-array of the camera used to record the OKE/TKE data. The dimensions of I4 were approximately 14.3 mm wide by 5.1 mm high. The camera subarray used to record data was 16.64 mm wide by 0.52 mm high.

B. Data Processing

The fast frame rate camera can produce large quantities of data quickly; for example, 10 seconds of data from the 1280×10 pixel sub-array with 2×8 binning and 1 kHz acquisition rate produces several hundred megabytes of data. Two data storage and analysis approaches were tested, using ascii (‘.asc’) and raw (‘.dat’) data file formats. In Andor Solis, writing .dat files to disk was found to be around 10-20× quicker than storing the data in the .asc format.

Python scripts were used for processing the camera data, and a similar time savings using the .dat file format was evident. With an equivalent series of processing steps, .dat files were analyzed >100× faster than .asc files. The Python script used for .dat file processing is shown below:

```
## bin_reader.py
import numpy as np
import matplotlib.pyplot as plt
import time

file = 'DIM_10K_.dat' # file name
w = 1280 # array width in pixels, 2x bin
h = 10 # array height in pixels, 8x bin
num = 10000 # number of images acquired

# init. arrays for even and odd image data
odd = np.zeros(w)
even = np.zeros(w)

# start timer
t0 = time.time()

# read in file with appropriate encoding
b = np.fromfile(file, dtype = np.int32)

t1 = time.time()
c = np.reshape(b, (num, h, w))
```

```
# sum along the array height
d = np.sum(c, axis=1)

# coadd images
for i in range(num):
    if i % 2 == 0:
        even += d[i,:]
    else:
        odd += d[i,:]

# perform subtraction, normalization
if np.max(even) > np.max(odd):
    diff = (even-odd)/odd
else:
    diff = (odd-even)/even

t2 = time.time()
print 'Read:', np.round(t1-t0, 3)
print 'Process:', np.round(t2-t1, 3)

# save processed data to txt file
np.savetxt('%s_diff.txt' % file, diff)

# plot results
plt.subplot(2,1,1)
plt.plot(even, label='Even')
plt.plot(odd, label='Odd')
plt.xlabel('Pixels (2x bin)')
plt.ylabel('# photons (counts)')
plt.legend(frameon=False)
```

```
plt.subplot(2,1,2)
plt.semilogy(diff, label='Diff')
plt.xlabel('Pixels (2x bin)')
plt.ylabel('Signal (a.u.)')
plt.legend(frameon=False)
plt.show()
plt.close()
```

C. Diiodomethane OKE Response

The OKE response of diiodomethane (CH_2I_2) was measured using the single shot apparatus, with similar results to bromoform achieved.

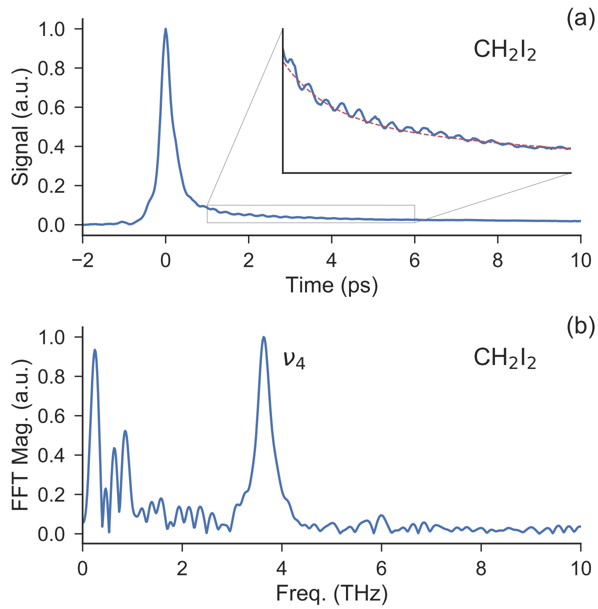

FIG. 2. (a) Diiodomethane OKE response measured using the echelon technique (N=10,000 shots). The oscillatory molecular coherences are shown in the inset, along with the orientational response fit. (b) Fourier transform of the fit residual reveals the ν_4 Raman mode at 3.65 THz.

D. Solvent OKE Responses: Stage vs. Echelon

The six solvents measured using the single shot echelon and stage scan techniques are shown below in Fig 3, with the difference (same scale, offset -0.2) between the two data sets shown to demonstrate the degree of agreement between the two techniques. Some small diffraction artifacts and irregularities are present in the electronic response regime, which is defined as the few hundred femtosecond region around the signal maximum. The longer picosecond scale molecular orientational responses were found to agree well between the two techniques.

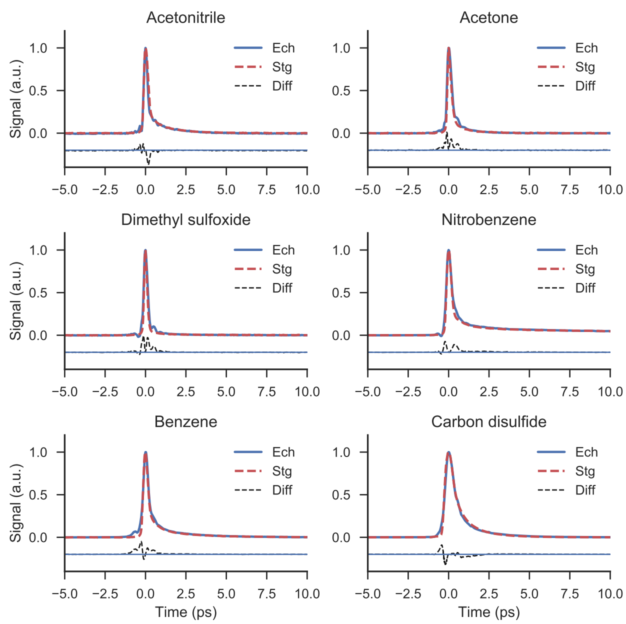

FIG. 3. Comparison plots of the six solvents investigated by OKE, demonstrating the good agreement between the two techniques across a range of response profiles. The echelon data consist of 10,000 laser shots (10 seconds), the stage scan data 45,000 laser shots (45 seconds).

E. Calculation of the Heterodyne and Homodyne Components in the Single Shot OKE Response

The single shot OKE responses of the six solvents measured in this study were decomposed into heterodyne and homodyne components using an algebraic solver written in Python. First, the difference signal Y and background signal E_{LO}^2 were extracted from the N=10,000 shot data set. These two 1280×1 vectors were then used as inputs to a Python symbolic solver which found the roots X to Eq. 4, where $X = E_{sig}$. In Fig 4, the heterodyne and homodyne components are shown for each solvent.

$$Y - X^2 + 2XE_{LO} = 0 \tag{2}$$

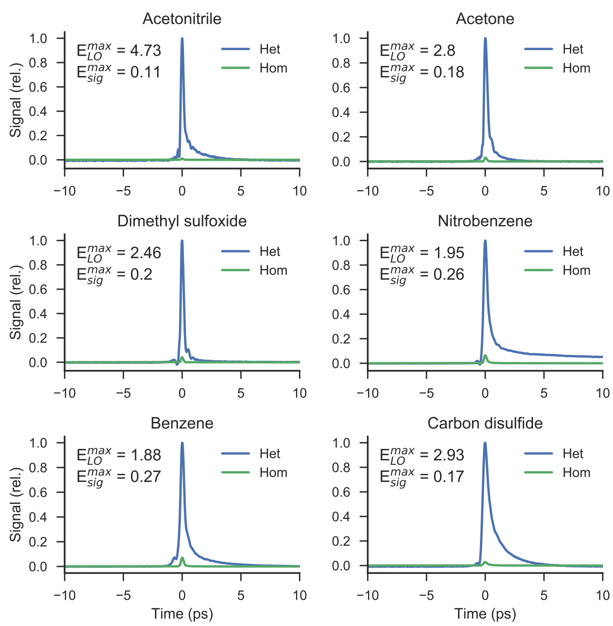

FIG. 4. The heterodyne and homodyne components of the single shot OKE responses of six solvents investigated in this study. The values in the upper left-hand corners specify the maximum relative magnitudes of the calculated E_{LO} and E_{sig} fields, demonstrating the $E_{LO} \gg E_{sig}$ condition for linear heterodyne detection.

F. Quadratic Scaling of OKE Signal

To verify the nonlinear nature of the observed OKE signal, a series of stage scan measurements were performed on CS_2. Neutral density filters were used to attenuate the pump beam power. The relative pump electric field strength of the measurements were calculated by taking the square root of the fractional transmission through each neutral density filter used. Plotting the relative electric field strength against the peak of the CS_2 signal yielded a quadratic relationship, as required for a nonlinear (i.e. $\vec{E}^2_{pump}$ dependent) signal.

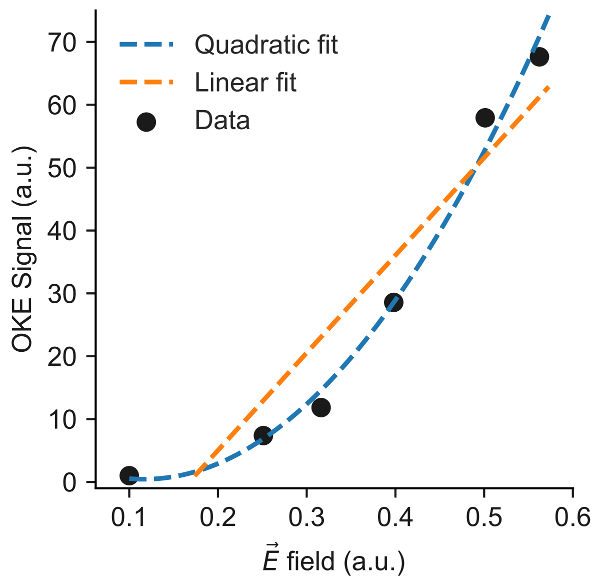

FIG. 5. The peak of the CS_2 OKE signal is plotted as function of the relative pump electric field strength. Data were taken using the stage scan technique, and neutral density filters were used to adjust the intensity of the transmitted pump. A quadratic relationship best fits the data, in contrast to a linear fit, and confirms the nonlinear origin of the OKE signal.